Multifractality and Multifractal Phase Transitions in Turbulence

Term Paper for Physics 464

Sébastien Boutet

Department of Physics, University of Illinois at Urbana-Champaign

May 2^{nd} 2000

Abstract

In this paper, the problem of fully developed turbulence is discussed using the formalism of multifractals. After an introduction of the subject matter of fluid dynamics and turbulence, a treatment of the Kolmogorov theory of turbulence is given, followed by a discussion of energy cascades. The multifractal formalism is then introduced and applied to the study of intermittency in turbulence. Scaling behavior of the velocity and dissipation fields in turbulent flows are discussed throughout this paper, always keeping experimental results in perspective. A presentation of the concepts of multifractal phase transitions is given to conclude the paper.

1 Introduction

The problem our fluid turbulence as puzzled the minds of scientists for almost four centuries. Leonardo da Vinci himself sunk its teeth into the problem a long time ago. Turbulence has even inspired the minds of poets. Despite all the efforts over the years, the solution is still elusive. An entire slew of techniques have been used to try and solve the problem. An extensive review of all the recent work in the field was recently published by Sreenivasan [1]. The interested reader is referred to this review. In this paper, we shall not even attempt to mention the different approaches used by many people. We will look at only one subfield of turbulence. Using the framework of multifractals, we will attempt to describe what is known as fully developed turbulent. Interestingly, some recent publications have suggested that such fully developed turbulence might not even exist. The interested reader is referred to [1].

In this paper, we will first introduce some basic concepts of fluid dynamics, before we actually define the phenomena of turbulence itself. This will be followed by an almost mandatory treatment of the Kolmogorov theory and energy cascades. We will then discuss fractals and multifractals as well as how they can be used to model intermittency in turbulence, concluding with a treatment of multifractal phase transitions.

2 Basics of Fluid Mechanics

We start by introducing some basic aspects of the theory of fluid dynamics which are necessary for the development of a theory of turbulence. We first make an assumption which will hold for our entire discussion. We assume that all the length scales under investigation are much larger than the mean free path of the fluid particles. Under this condition, we can treat the entire fluid as a continuum and not worry about the actual atoms present. The theory thus derived will be valid for all structures larger than the mean free path, which is the well known classical limit of thermodynamics. This means we need only concern ourselves with a classical theory of fluid turbulence and we can completely forget about quantum mechanics. The fluid is then expected to obey Newton's law of motion. Rewriting Newton's second law for a small volume contained in a continuum yields the celebrated Navier-Stokes equation [2] which has been known since the time of Navier(1823).

$$\partial_t \vec{v} + \vec{v} \cdot \nabla \vec{v} = -\nabla p + \nu \nabla^2 \vec{v} + f \tag{1}$$

where $\vec{v}$ is the velocity of the fluid, ν is the kinematic viscosity, p is the pressure and f is any external force. This equation on its own is not sufficient to specify the fluid flow. Extra constraints are required. One such constraint is the fact that the total quantity of fluid must be conserved. We then have the continuity equation

$$\partial_t \rho + \vec{\nabla} \cdot (\rho \vec{v}) = 0 \tag{2}$$

where ρ is the density of the fluid. We will be interested below in a theory of incompressible fluids with a uniform densities. The continuity equation (2) then reduces to $\vec{\nabla} \cdot \vec{v} = 0$, which is known as the incompressibility condition. Often this incompressibility condition and Equation (1) are taken together and referred to as the Navier-Stokes equations. Along with suitable initial and boundary conditions, these equations are "believed" to represent any fluid flow. We must emphasize here on the word believed since existence and uniqueness of the solution are yet to be proven in more the 2 dimensions. The difficulty comes from the second term in the equation, known as the nonlinear term. The fourth term is known as the viscous term.

It is convenient to write the Navier-Stokes equation in terms of dimensionless variable. This can be achieved via the following transformation : $\vec{x'} = \frac{\vec{x}}{L}$, $\vec{v'} = \frac{\vec{v}}{U}$, $p' = \frac{p}{U^2}$ and $t' = \frac{tU}{L}$. Here, L and U are characteristic length and velocity scales of the flow respectively. The non dimensional Navier-Stokes equation now reads

$$\partial_{t'} \vec{v'} + \vec{v'} \cdot \nabla' \vec{v'} = -\nabla' p' + \frac{1}{Re} \nabla'^2 \vec{v'} \tag{3}$$

where we dropped the external forcing term and introduced the Reynolds number $Re = \frac{LU}{\nu}$. The Reynolds number is a dimensionless parameter which turns out to be very important in fluid mechanics. As can be seen from above, the dimensionless Navier-Stokes equation (3) depends only on Re. It is universal for a specified value of Re and identical boundary conditions, which means that Re is the only control parameter. Then two different flows with the same geometry and same Re will have identical dimensionless solutions. Hence, one characterizes a fluid flow by its Reynolds number only instead of specifying its mean velocity for example. The Reynolds number also has a physical significance. It is the ratio of the nonlinear or inertial term to the viscous term. In the large Re limit, the dimensionless Navier-Stokes equation becomes

$$\partial_{t'}\vec{v'} + \vec{v'} \cdot \nabla' \vec{v'} = -\nabla' p' \tag{4}$$

and the region where this equation is valid is known as the inertial range since the dynamics are dominated by the inertial term. Notice that the large Re limit is equivalent to the low viscosity limit ($\nu \to 0$), an important limit in turbulence. In the low Re limit or when the viscosity becomes large, the dissipation gets more important and the Navier-Stokes equation becomes

$$\nabla' p' = \frac{1}{Re} \nabla'^2 \vec{v'} \tag{5}$$

The regime dominated by the viscous term is known as the dissipation range.

3 Turbulence

For low Reynolds number, a fluid flow will be smooth and uniform or what is known as laminar. As Re is increased, by either reducing the viscosity, increasing the mean velocity or the size of the system, the flow becomes increasingly more wild or turbulent. We here look at an example taken from [3] and [4] to see what the transition to turbulence looks like. Figure 1(a) shows a flow past a cylinder at $Re = 0.16$. In the case of a flow past a cylinder, the characteristic length scale in Re is taken to be the radius of the cylinder. At such low Reynolds number, the flow is very uniform and displays some symmetries. The flow is seen to be time invariant, invariant under up-down reversal and almost invariant under left-right reversal. Except for the left-right symmetry, which is broken by the nonlinear term of the Navier-Stokes equation by introducing a preferred direction of the flow, all these symmetries are allowed by the Navier-Stokes equation. However, as we increase the Reynolds number, those symmetries are successively broken. This can be seen on Figure 1(b) which shows Kárman vortex streets which clearly break the continuous time invariance of the flow, replacing it by a discrete time invariance. As we increase Re even more, the flow becomes even more turbulent. Figure 1(c) now shows the flow behind two cylinders. The presence of the second cylinder does not affect the point we want to make here. One should note that at such a high Reynolds number, the flow looks "uniform" when it is sufficiently coarse grained. That is the symmetries have been restored but only in a statistical sense. Every point in time and in space for a region behind the cylinder looks the same statistically. This allows us to formulate the following definition of fully developed turbulence. When some or all the symmetries of the Navier-Stokes equation are restored, from a statistical point of view, the turbulence is then said to be fully developed. All the models which will be discussed below apply to fully developed turbulence.

There are many known symmetries of the Navier-Stokes equation and we shall take here a close look three of them which are of special interest. The first two are invariance under space and time translation as discussed above and can be visualized on Figure 1. These symmetries are relevant because of the way measurements on fluid flow are usually made. One cannot have sensors at every point along the flow since those would disrupt the flow. It is then impossible to measure the velocity at all points at the same time. The common practice is to sample the flow at a single point along it and collect a time series of data. If the time translation symmetry holds and the space translation also holds approximately, one can then transform the time series into a space series by the simple transformation $\ell = Ut$ where U is the mean velocity of the flow. Clearly, this is justified only if the flow is statistically the same for all spatial

and time translation within the series. This transformation from time to space is known as Taylor's hypothesis. It is only justifiable for low turbulent intensity since at high intensity, the time it takes for a structure to travel from its original position to the sensor will be longer than the time it takes the flow to deform this structure. In such a case, the time series will not yield the same measurement as a real spatial snapshot (See [3] for details).

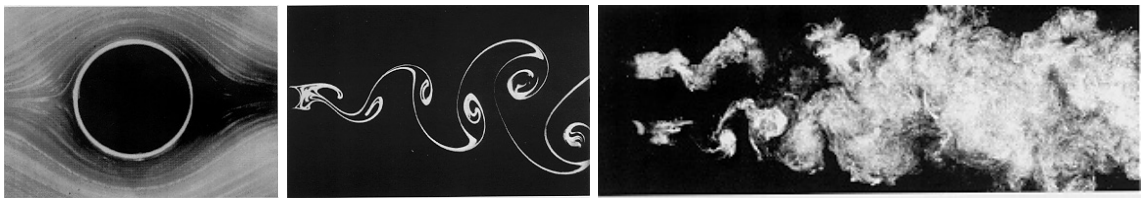

Figure 1: (a) Uniform flow around a cylinder at $Re = 0.16$. (b) Kárman vortex streets behind a cylinder at $Re = 140$. (c) Turbulant wake behind 2 cylinders at $Re = 1800$. Pictures taken from [3].

The third symmetry, which will be the most important one for us, is the scaling symmetry. That is if we rescale the parameters such that

$$t, \vec{x}, \vec{v} \longrightarrow \lambda^{1-h} t, \lambda \vec{x}, \lambda^h \vec{v} \tag{6}$$

then the Navier-Stokes equation looks the same, almost! In fact, under this transformation, every term in Equation (1) or (3) picks up an extra factor of λ^{2h-1} except for the viscous term which gets multiplied by λ^{h-2}. This would mean that only $h = 1$ is an acceptable scaling exponent. However, in the limit of low viscosity or large Reynolds number, we can neglect the viscous term and there is an infinite number of allowed scaling groups labeled by the scaling exponents h. This will be important when we discuss scaling in the inertial range in the framework of Kolmogorov's theory, as well as when we discuss multifractals.

It was pointed out earlier that the Navier-Stokes is believed to represent any fluid flow. Then it also probably contains within it all there is to know about turbulence. However, the very large range of scales which display structure, as well as the extreme sensitivity to initial conditions makes it impossible to solve the Navier-Stokes equation deterministically. One then resorts to a statistical stochastic treatment of turbulence. Modeling a deterministic equation like the Navier-Stokes equation by random or stochastic statistical models can be justified (see [3]).

4 Old Theory of Turbulence

We shall here motivate and describe the old theory of turbulence, leading to the Kolmogorov theory and the Richardson cascade model.

4.1 Energy Budget Scale-by-Scale

We start by deriving an exact result known as the energy budget scale-by-scale from the Navier-Stokes equation. We define the high and low pass filtered functions

$$\begin{aligned} f_K^{>}(\vec{r}) &\equiv \sum_{k \geq K} \hat{f}_k e^{i\vec{k}\cdot\vec{r}} \quad \text{high pass} \\ f_K^{<}(\vec{r}) &\equiv \sum_{k \leq K} \hat{f}_k e^{i\vec{k}\cdot\vec{r}} \quad \text{low pass} \end{aligned} \tag{7}$$

where $\hat{f}_k$ is the discrete Fourier transform of $f(\vec{r})$ and $f(\vec{r}) = f_K^>(\vec{r}) + f_K^<(\vec{r})$. We can define the low pass operator $P_K : \vec{v}(\vec{r}) \to \vec{v}_K^<(\vec{r})$ and act on the Navier-Stokes equations (1) with this new operator. We then get

$$\partial_t \vec{v}_K^< + P_K(\vec{v}_K^< + \vec{v}_K^>) \cdot \vec{\nabla}(\vec{v}_K^< + \vec{v}_K^>) = -\nabla p_K^< + \nu \nabla^2 \vec{v}_K^< + f_K^< \tag{8}$$

$$\vec{\nabla} \cdot \vec{v}_K^< = 0 \tag{9}$$

We take the scalar product of Equation (8) with $\vec{v}_K^<$ and than take ensemble averages. Then, using the facts that P_K is a projection operator, commutes with ∇ and ∇^2 and is self-adjoint (see [3]), we get

$$\partial_t \underbrace{\frac{1}{2}\left\langle \left|\vec{v}_K^<\right|^2 \right\rangle}_{\mathcal{E}_K} + \underbrace{\left\langle \vec{v}_K^< \cdot \left(\vec{v}_K^< \cdot \nabla \vec{v}_K^>\right)\right\rangle + \left\langle \vec{v}_K^< \cdot \left(\vec{v}_K^> \cdot \nabla \vec{v}_K^>\right)\right\rangle}_{\Pi_K} = -2\nu \underbrace{\frac{1}{2}\left\langle \left|\vec{\omega}_K^<\right|^2 \right\rangle}_{\Omega_K} + \underbrace{\left\langle f_K^< \cdot \vec{v}_K^> \right\rangle}_{F_K} \tag{10}$$

where $\mathcal{E}_K$ is the energy contained in structures having wavevectors $k < K$, Ω_K is called the enstrophy for $k < K$, F_K is the energy injection for $k < K$ and Π_K is the energy flux through the structures of wavevectors $k < K$. The terms are interpreted as follows : F_K is the energy injection at scales down to $\ell = K^{-1}$, $-2\nu\Omega_K$ is the energy dissipated at scale ℓ, $\partial_t \mathcal{E}_K$ is the total change in energy at scale ℓ and Π_K is the energy flux coming from larger to smaller scales. Usually, the energy injection occurs only at the largest scales (integral scale) and the dissipation occurs only at the smaller scales (low Re limit or dissipation range). Then, in the inertial range defined earlier, we have $F_K = -2\nu\Omega_K = 0$ and we get that the change in energy only comes from a redistribution of energy from large to small scales. The main thing to notice here is that the flux (Π_K) arises from the nonlinear term of the Navier-Stokes equation. Hence, we conclude that it is this nonlinear term which causes this redistribution of energy.

4.2 Kolmogorov's 1941 Theory (K41)

In 1941, A.N. Kolmogorov published a series of three papers [5], [6], [7] in which he elaborated a theory of fully developed turbulence based on a few simple reasonable assumptions. He derived what is known as the four fifth law from simple arguments. Some of these arguments have since been found to not be quite correct but the important end results have been shown to be valid even when less stringent assumptions are made. The Kolmogorov theory, often referred to as K41, is the starting point of any more refined theory of turbulence and we shall review it here. We will not derive the results but merely state them while emphasizing on the underlying physical assumptions made. It is important to understand the K41 theory since it is its apparent flaws that prompted the study of intermittency and the development of multifractal models of turbulence.

We shall make here three key hypotheses about fully developed turbulence. Those are not assumptions made by Kolmogorov himself. In his work, he assumed universality, meaning that all turbulence behaves in an identical fashion no matter how it was generated, i.e. independent of the boundary conditions on the flow. This argument has been rejected by Landau and cannot be expected to hold true in general (see [3]). The assumptions we make here are more general and are still consistent with Kolmogorov's original idea. These assumptions were taken directly from [3].

> (i) - In the limit of infinite Reynolds number, all the symmetries of the Navier-Stokes equation, usually broken by the mechanism producing the turbulent flow, are restored in a statistical sense at small scales and away from boundaries.

This deserves some comments. First of all, by small scales it is meant scales that are small compared to the size(ℓ_0) of the object producing the turbulence. We call this scale ℓ_0 the integral scale of the flow and it is the length scale used in the Reynolds number. The length scale of observation also cannot be so small as to reach the Kolmogorov dissipation scale. We are then concerned with only what we defined earlier as the inertial range. It is important to recall that only the time translation symmetry is expected

to be exact in fully developed turbulence. Other symmetries like space translation invariance will only hold for certain ranges of scales and only at certain positions in the flow. Here and below we will be considering the velocity increments defined as

$$\delta\vec{v}(\vec{r},\vec{\ell}) \equiv \vec{v}(\vec{r},\vec{\ell}) - \vec{v}(\vec{r}) \tag{11}$$

The space translation symmetry, or the small scale homogeneity implies that

$$\delta\vec{v}(\vec{r}+\vec{\rho},\vec{\ell}) \stackrel{\text{law}}{=} \delta\vec{v}(\vec{r},\vec{\ell}) \tag{12}$$

where equality in law means they are equivalent statistically. So the velocity increments look the same, from a statistical point of view, everywhere in the inertial range of the turbulent flow.

(ii) - The flow is self-similar at all scales and possesses a single scaling exponent h.

It was mentioned above that in the inertial range, an infinite number of scaling exponents h are allowed. However, we postulate here that the flow is characterized by only one such exponents to be determined later. Then if we rescale the scale of observation $\ell \to \lambda\ell$, the velocity increment scales as λ^h.

$$\delta\vec{v}(\vec{r},\lambda\vec{\ell}) \stackrel{\text{law}}{=} \lambda^h \delta\vec{v}(\vec{r},\vec{\ell}) \tag{13}$$

(iii) - The turbulent flow has a finite non-vanishing mean rate of dissipation per unit mass (ε).

This simply represents the fact that experiments all seem to show that there is a non zero rate of dissipation when the viscosity goes to zero. If we take a particular turbulent flow and keep its root mean square velocity as well as its integral length scale ℓ_0 constant and make the viscosity as small as possible, then the rate of dissipation ε goes to a constant finite value. This might come as a surprise since one would expect no dissipation when there is no viscosity but all experiments tend to show finite dissipation.

From these three assumptions, it is possible to derive Kolmogorov's four fifth law, which goes as follows [3].

$$S_3(\ell) = \left\langle \left(\delta\vec{v}_{\parallel}(\vec{r},\vec{\ell})\right)^3 \right\rangle = -\frac{4}{5}\varepsilon\ell \tag{14}$$

where the function $S_3(\ell)$ is called the (longitudinal) third order structure function. This result is exact not only under the assumptions made but also for all homogeneous isotropic turbulence. The constant $-\frac{4}{5}$ is universal. We can use Equation (14) to determine the unique scaling exponent h. We have seen from Equation (13) that the velocity increment scales as λ^h. Thus, the left hand side of Equation (14) scales as λ^{3h} while the right hand side scales as λ. For the equation to be consistent, we require $h = \frac{1}{3}$.

We can note here that Kolmogorov's original assumption of universality said that all structure functions of all orders p could be written as $S_p = C_p\varepsilon^{p/3}\ell^{p/3}$ where all the C_p's are universal constants. This was however shown by Landau to be incorrect [3]. It is believed that some form of scaling similar to that exists but the constants C_p cannot be universal. We will come back to that when discussing intermittency.

An important experimental result is that the power spectrum of turbulence behaves as a power law in the wavevector k in the inertial range. Figure 2(a) shows one such spectrum and Figure 2(b) an example of structure function. The Kolmogorov theory implies that the power spectrum is given by $E(k) \sim \varepsilon^{2/3}k^{-5/3}$ where k is the wavevector. This relation was first written down by Obukhov [8], [9] in 1941 and can be easily obtained by simple dimensional analysis but can also be obtained from the following statistical relation between the second order structure function and the power spectrum. If $E(k) \propto k^{-n}$ then $S_2 \propto (\ell)^{n-1}$. We get from Kolmogorov's theory that $h = n - 1 = \frac{2}{3}$, hence $n = 5/3$ and the spectrum behaves as $k^{-5/3}$. Figure 2 shows that there seems to be an inertial range where these power laws are valid. We also mentioned earlier that the data is usually collected in the time domain

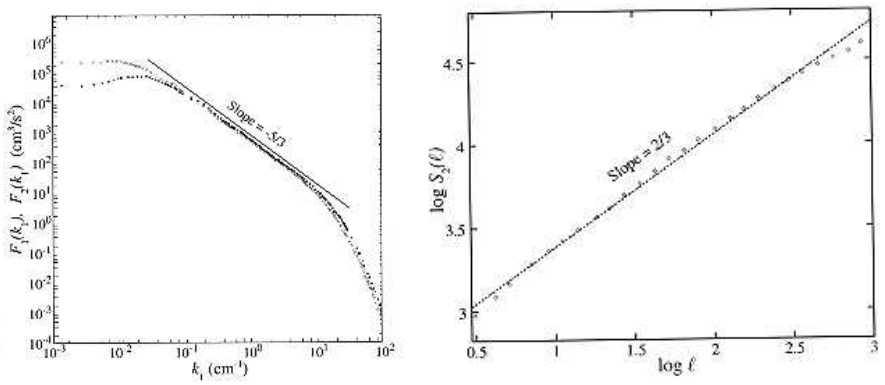

Figure 2: (a) Typical example of a power spectrum for the streamwise component(white circles) and lateral component (black circles) of the velocity fluctuation in the time domain for a jet at $Re = 626$. (b) Typical example of a second order structure function of wind tunnel data in the time domain. Some scaling range can be observed for both. Pictures taken from [3].

and not in the space domain. Using the Taylor hypothesis, when valid, we can modify the above results to get the second order structure function and the spectrum in the time domain. Hence

$$\begin{aligned} E(k) \propto k^{-5/3} &\xrightarrow{\text{Taylor}} E(\omega) \propto \omega^{-5/3} \\ S_2(\ell) \propto \ell^{2/3} &\xrightarrow{\text{Taylor}} S_2(t) \propto t^{2/3} \end{aligned} \tag{15}$$

4.3 Richardson Cascades

A simple picture of turbulence representing the results obtained so far is given by the energy cascade model known as the Richardson cascade. Figure 3 below depicts the process. As we mentioned earlier, the energy injection in turbulence occurs mostly at the largest scales, near the integral scale. The dissipation on the other hand, as shown, occurs at the smallest scales, near the Kolmogorov scale (η). For the intermediate scales, the nonlinear term of the Navier-Stokes equation redistributes the energy from the larger scales without dissipation (according to K41). The larger eddies break off into smaller eddies, which then break up into even smaller ones and so on until the dissipation scales are reached. At every step of the cascade, the size of the new eddies are related to the old ones by $\ell_{new} = r\ell_{old}$ where $r = 1/2$ is a common choice. It is important to notice that this model assumes that all the space occupied by the mother eddies is completely filled by the daughter eddies. If this was really the case, the K41 theory would be exactly true in the inertial range. However, there is no reason why this should be so and non-space filling models can be developed to model intermittency. Those seem to model the data better and are called multifractal models.

5 Fractals and Multifractals

Before we discuss intermittency and how multifractals can be used to describe it, we should digress shortly and introduce some basic concepts of fractals and multifractals. A fractal set can be loosely defined as a set which shows irregularity on all scales [10]. The most common example of this is the measure of a

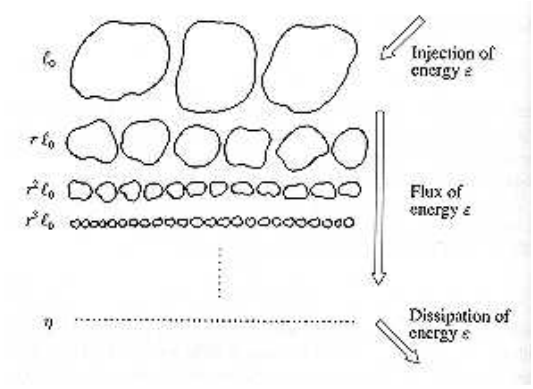

Figure 3: The Richardson cascade model according to K41 theory. Notice that at each step the eddies are space filling. Picture taken from [3].

coastline. If one uses an increasingly small length of reference or measurement and looks at the shoreline with more and more precision, it seems like the total length of the shoreline increases infinitely. Thus fractal measures depend on the scale of observation. We shall talk here only about random fractals since deterministic or exact fractals do not seem to make sense in the context of turbulence. For example, in the Richardson cascade model discussed above, there are no good reason to believe that every eddy breaks off exactly in half at each step of the cascade. One could imagine that on average, eddies split roughly in half but each realization does not have to have a ratio of 1/2. There is then a need to take averages, hence a need for random fractals (see [10]).

5.1 Homogeneous Random Fractals

We here look at a simple example to see what is meant by random fractals and how we define the fractal dimension. Figure 4(a) below shows the process we wish to describe. A square is split into four identical squares only two of which are full or active. One can think of these boxes as eddies being either active or inactive. We can define a mass ratio β between the two steps. In this case, $\beta = \frac{2}{4} = \frac{1}{2}$. As shown, there are different combinations possible for which two squares are occupied. If this choice is made at random, we have a random fractal. This particular fractal, shown after two iterations on Figure 4(b) is an homogeneous fractal since β is kept constant at each step of the process. The fractal dimension D is given by $D = d + \frac{\log \beta}{\log 2}$ where d is the dimension of the space which supports the fractal (in this case $d = 2$). This dimension D can be found from a single iteration. We have $2^d\beta$ new elements, each of size $1/2$, hence we get $2^d\beta(1/2)^D = 1$.

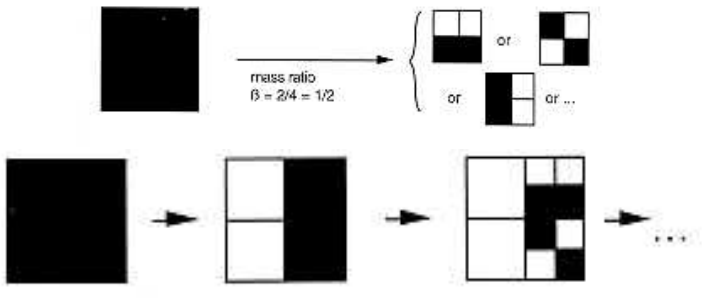

Figure 4: (a) (Top picture) This shows the generator of the random fractal. (b) (Bottom picture) Shows the random fractal generated after 2 iterations. Pictures taken from [10].

5.2 Heterogenous Fractals

This is the type of fractals which is of most interest to turbulence. We look at a similar example as the one above but we now let β be a random variable satisfying $0 < \beta < 1$. What we obtain is an heterogeneous random fractal. The fractal dimension is now $D = d + \frac{\log\langle\beta\rangle}{\log 2}$ where $\langle\beta\rangle$ is the average value of β. The process is shown on Figure 5.

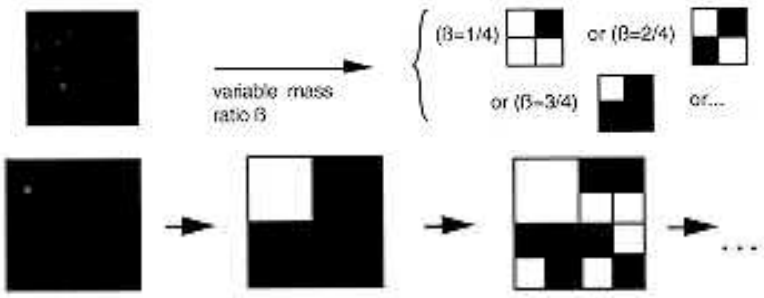

Figure 5: (a) (Top picture) This shows the heterogeneous generator. Notice the different β's. (b) (Bottom picture) The heterogeneous fractal generated after 2 iterations. Notice the difference between the heterogeneous and homogeneous case. Pictures taken from [10].

The relevance of fractals to turbulence comes from the scale invariance or self-similarity of fractals. For fractal measures $M(L)$, we get under rescaling that $M(bL) = b^D M(L)$. This kind of scaling is what we encountered earlier when discussing the scaling behavior of structure functions in turbulence flows.

We now turn to multifractals which are more easily introduced within a discussion of intermittency. Hence, we move directly on to a discussion of intermittency.

6 Intermittency in Turbulence

The K41 theory tells us that in the inertial range, the velocity function is a random function which scales as ℓ^h under coarse graining operations on the length scale of observation. This means that the velocity profile under K41 theory is self-similar, i.e. it looks the same (statistically) at all scales in the inertial range. Such a self-similar function is by definition not intermittent. An intermittent function is one that is "on" or not zero only a certain fraction of the time. An example of this in turbulence could be the high pass filtered velocity function defined earlier. The high pass filter will keep only the structures that have wavevectors larger than some vector K_1, hence the structure with $\ell < \ell_1$. If we tune the value of K_1 to correspond to the Kolmogorov dissipation scale η, we can filter out all the data which is not in the dissipation range. The dissipation is not expected to be uniform because different structures of different size should dissipate differently. The signal will then vary a lot in time and look very intermittent. There is very little doubt that intermittency does indeed take place in the dissipation range and that fact does not violate the K41 theory which applies only to the inertial range. We shall not say anymore about the dissipation range intermittency. Instead, we will focus our attention on intermittency models for the inertial range of fully developed isotropic homogeneous turbulence. In particular, we will look at multifractal models based on the local velocity and multifractal models based on the local rate of dissipation and see how the two are related.

6.1 Preliminary Discussion

We shall assume from now on that velocity structure functions of all order exist. This might not be the case since for long tails of the probability distribution, moments of order higher than a critical value will diverge. We will look at those long tails when we discuss multifractal phase transitions. But for now we simply assume finite structure functions. Furthermore, we shall assume that all the structure functions follow a power law behavior : $S_p(l) = \langle(\delta v(\ell))^p\rangle \propto \ell^{\zeta_p}$ where the ζ_p's are called the exponents of the structure function. This is very similar to the K41 theory except that now the $\zeta_p \neq p/3$, with the restriction that $\zeta_3 = 1$, which should hold regardless of the validity of K41. This power law behavior as been shown to be reasonable for values of p up to 15 or 20. This is roughly to upper limit reachable from the finite size of the data sample. Larger and larger samples are needed to evaluate higher order moments. One should keep in mind that all the discussion below is only valid for isotropic, homogeneous, fully developed turbulence where the finite dissipation limit ($\lim_{\nu\to 0}\varepsilon = \text{const}$) holds. One exact result in intermittency can be obtained for the functional form of $\zeta(p)$. Frisch [3] shows that $\zeta(p)$ has to be a convex up non decreasing function of p.

6.2 Models based on the velocity

6.2.1 The β-model

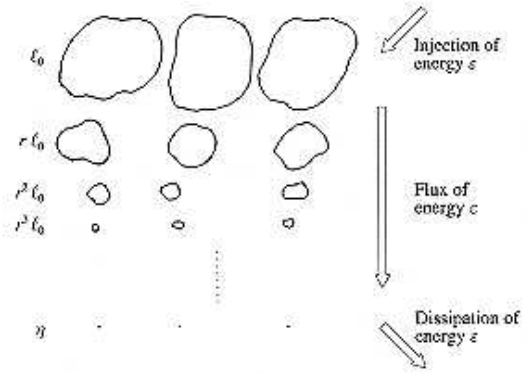

Figure 6: Energy cascade according to the β-model. Notice that with each step the eddies become less and less space filling. Picture taken from [3].

The β-model comes from a simple modification of the Richardson cascade discussed earlier. Figure 6 illustrates the situation. The only difference between this picture and the one shown on Figure 3 is that the daughter eddies are not fully space filling. One can see this as following. The mother eddies split up in the exact same way as before but now only a fraction of the daughter eddies are active (in the same way as our simple fractal example earlier). The fraction of the space occupied, or the fraction of space active at scale $\ell = r^n\ell_0$ is

$$p_\ell = \beta^n = \beta^{\frac{\log(\frac{\ell}{\ell_0})}{\log r}} = \left(\frac{\ell}{\ell_0}\right)^{3-D} \tag{16}$$

where $3 - D \equiv \frac{\log\beta}{\log r}$. The value of r is once again usually chosen to be $1/2$ for simplicity. The parameter D is recognized as being the fractal dimension. In the case above, we worked in three dimensions, hence the factor $3 - D$. We can extend this to d dimensional space and get $d - D \equiv \frac{\log\beta}{\log r}$. We can identify this quantity as the codimension of the singularities as we will see later. We can now use simple

phenomenological arguments to see how the K41 theory is modified. The energy at scale ℓ is given by $\sim v_\ell^2$ times the probability p_ℓ that the scale ℓ is active. Then

$$E_\ell \sim v_\ell^2 p_\ell = v_\ell \left(\frac{\ell}{\ell_0}\right)^{3-D} \tag{17}$$

We can get the energy flux from

$$\Pi_\ell = \frac{E_\ell}{t_\ell} = \frac{v_\ell^3}{\ell}\left(\frac{\ell}{\ell_0}\right)^{3-D} \tag{18}$$

where $t_\ell = \frac{\ell}{v_\ell}$ is the eddy turnover time, or the time taken by an eddy of size ℓ to undergo significant distortion. Under our basic assumption that at high Reynolds number $\Pi_\ell = \varepsilon$, a constant, we get from Equation (18)

$$v_\ell \sim v_0 \left(\frac{\ell}{\ell_0}\right)^{\frac{1}{3}-\frac{3-D}{3}} \tag{19}$$

This is equivalent to saying that the velocity scales as $h = \frac{1}{3} - \left(\frac{3-D}{3}\right)$. We notice here that if $D = 3$, we get back, as we should, the K41 value of $h = 1/3$. We now use the result of Equation (19) to calculate the structure functions. There are two contributions : the value of v_ℓ^p and the fraction p_ℓ of volume occupied. We then get for the exponents ζ_p

$$\zeta_p = \frac{1}{3} + (3-D)\left(1 - \frac{p}{3}\right) \tag{20}$$

We again recover the K41 result when the fractal dimension D is equal to the dimension of space ($D = 3$). We can use the value of the exponent of the second order structure function to calculate the power spectrum. We then see the $E(k) \propto k^{\left(\frac{5}{3}-\frac{3-D}{3}\right)}$ which is steeper than the Kolmogorov-Obukhov spectrum for $D < 3$. Some experiments do indeed measure spectra steeper than $k^{-5/3}$. It is worth noticing that the β-model yields a linear function of p for ζ_p, as does the K41 theory. The only differences are that the two models have different slopes and the β-model is linear plus a constant. A comparison of the two models can be seen on Figure 8.

6.2.2 The Bifractal Model

The simplest multifractal model one can think off is the bifractal model. We just saw that the β-model means that the velocity function has a scaling exponent h on a fractal set $\mathcal{L}$ of dimension D. We can extend the idea to a bifractal model by postulating the existence of two exponents, h_1 and h_2, belonging to sets $\mathcal{L}_1$ and $\mathcal{L}_2$ of dimensions D_1 and D_2. In this case it is simple to show that

$$\frac{S_p(\ell)}{v_0^p} = \mu_1 \left(\frac{\ell}{\ell_0}\right)^{ph_1+(3-D_1)} + \mu_2 \left(\frac{\ell}{\ell_0}\right)^{ph_2+(3-D_2)} \tag{21}$$

where μ_1 and μ_2 are constants of order unity and represent the relative weight of the two sets. We then have a superposition of two power laws. We are interested in the inertial range, for which the condition $\ell/\ell_0 << 1$ applies. The smallest exponent will thus dominate and the exponents ζ_p will be the smaller of the two given by

$$\zeta_p = \min(ph_1 + 3 - D_1, ph_2 + 3 - D_2) \tag{22}$$

The exponents are determined by which of the two types of singularities dominates. It is interesting to look at an example. We choose $D_1 = 3$ (K41 value) and $D_2 = D$, where $0 < D < 3$. Then for $p < 3$, the K41 singularities dominate while for $p > 3$, the second type takes over. The function $\zeta(p)$ is shown on Figure 7. One should notice the kink, or discontinuity in the slope at $p = 3$. This is an example of multifractal phase transition.

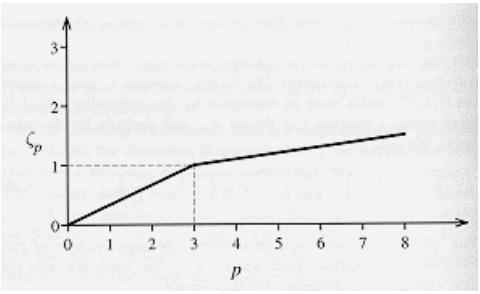

Figure 7: Exponents ζ_p for the bifractal model. The change of slope at $p = 3$ represents a multifractal phase transition. Picture taken from [3].

6.2.3 The Multifractal Model

One can readily extend the bifractal model to an infinite set of scaling exponents h. As we recall from our earlier discussion of the symmetries of the Navier-Stokes equation, such an infinite set is allowed in the inertial range. This however clearly violates the second assumption we made earlier in the context of the Kolmogorov theory. There, we assumed the existence of a single exponent. We can reformulate this assumption as follows (taken from [3])

> The turbulent flow is assumed to possess a range of scaling exponents $I = (h_{min}, h_{max})$. For each h in this range, there is a set $\mathcal{L}_h$ of fractal dimension $D(h)$ such that as $\ell \to 0$, $\frac{\delta v_\ell(\vec{r})}{v_0} \sim \left(\frac{\ell}{\ell_0}\right)^h$. The exponents h_{min} and h_{max} and the function $D(h)$ are postulated to be universal.

From this, one gets in a way similar to the bifractal case

$$\frac{S_p(\ell)}{v_0^p} \sim \int_I d\mu(h) \left(\frac{\ell}{\ell_0}\right)^{ph+(3-D(h))} \tag{23}$$

where the sum has been replaced by an integral over the entire range I. Once again, for small ℓ, the singularities with the smallest exponent will dominate. Once gets from a steepest descent calculation

$$\zeta_p = \inf_h(ph + 3 - D(h)) \tag{24}$$

where $\inf_h$ means the infimum of the function or set of points with respect to h. The relation in Equation (24) can be inverted to get

$$D(h) = \inf_h(ph + 3 - \zeta(p)) \tag{25}$$

and one recognizes Equations (24) and (25) as Legendre transforms of each other and since $\zeta(p)$ is convex up in p, $D(h)$ is convex up in h (see [3] for details).

A comparison of the models discussed so far and others to be discussed later can be made with the experimental data. This is shown on Figure 8. One can see that the data does not seem to display a kink as in the bifractal model. Also, the linear aspects of the K41 theory and the β-model do not seem to represent the data well above orders 6 or 8. However, it should be pointed out that this data is still not sufficient to completely dismiss any model, even the K41 theory. Many experimental problems could cause the deviations observed, the most important being the finite size of the data sample which implies unconverged statistics for higher order moments. Such a lack of convergence tends to bend the curve down for larger values of p. On Figure 8 is also shown a curve for the log-normal model which is a simple multifractal model we will discuss shortly.

6.3 Intermittency models based on the dissipation

6.3.1 Multifractal Dissipation

In a previous section, we used simple phenomenological arguments to find how the velocity field scales. One can go through a similar argument for the local dissipation rate at scale ℓ (ε_ℓ). If one assumes the existence of singularities as above, the following relation holds : $\frac{\varepsilon_\ell(\vec{r})}{v_0^3/\ell_0} \sim \left(\frac{\ell}{\ell_0}\right)^{\alpha-1}$. The analogy with the velocity case is clear. We have scaling exponents $\alpha - 1$ on sets $\mathcal{D}_\alpha$ of dimensions $F(\alpha)$. The analogue of the velocity structure functions are the moments of order q of ε. Then, we have

$$\langle \varepsilon_\ell^q \rangle \sim \left(\frac{v_0^3}{\ell_0}\right)^q \left(\frac{\ell}{\ell_0}\right)^{\tau_q} \tag{26}$$

The exponents τ_q are found in a similar fashion as the ζ_p. We can relate τ_q to $F(\alpha)$ by a Legendre transform

$$\begin{aligned} \tau(q) &= \inf_\alpha(q(\alpha-1)+3-F(\alpha)) \\ F(\alpha) &= \inf_q(q(\alpha-1)+3-\tau(q)) \end{aligned} \tag{27}$$

6.3.2 Relating velocity based and dissipation based multifractality

To do this, we need a result first derived by Kolmogorov and Obukhov in 1962 [11], [12]. The result relies on the fact that in K41 theory, $v_\ell \sim (\varepsilon\ell)^{1/3}$. One can replace ε by ε_ℓ and non-dimensionalize the velocity increment. If we assume that the non-dimensionalize velocity increments and the local rate of dissipation are statistically independent, we then get the following relations

$$h = \frac{\alpha}{3} \quad D(h) = F(\alpha) \quad \zeta_p = \frac{p}{3} + \tau_{p/3} \tag{28}$$

which relate both types of multifractality. It is not clear whether this assumption known as Kolmogorov's Refined Similarity Hypothesis is really justified but it has been studied experimentally in [13].

7 Multiplicative Random Cascades

A simple way to generate multifractal dissipation is by constructing what are known as multiplicative random cascades. As in the cascade models discussed so far, we start with a large eddy breaking up in equal parts of size $\ell/2$ and so on. For each of these new eddies, the dissipation variable is assigned a random weight $W \geq 0$ which also obeys the constraints $\langle W \rangle = 1$ and $\langle W^q \rangle < \infty$ for all positive values of q. After n steps, the size of the eddies is $(\ell_0/2)^n$ and the value of the local dissipation variables are given by $\varepsilon_\ell = \varepsilon W_1 W_2 \cdots W_n$. The W's are independent and uniformly distributed. One can readily see that some combinations of W's will give rise to values of ε_ℓ which are very large while some others will be very close to zero ($\mathcal{O}(2^{-n})$). This creates a very intermittent field for ε_ℓ. Such a cascade can be shown to lead to power laws for the moments of ε_ℓ such that

$$\begin{aligned} \langle \varepsilon_\ell^q \rangle &\sim \varepsilon^q \left(\frac{\ell}{\ell_0}\right)^{\tau_q} \\ \tau_q &= -log_2\langle W \rangle \end{aligned} \tag{29}$$

If we take a simple two state model for W so that $W = 1/\beta$ with probability β and $W = 0$ with probability $1-\beta$, it can be shown using the Refined Similarity Hypothesis that we get back the β-model previously obtained (see [3]). We can also develope a more involved model known as the log-normal model. In the

case, we assume that $W = 2^{-m}$ where m is a Gaussian (or so-called normal) variable. This is equivalent to saying that the log of W is a Gaussian variable, hence the name log-normal. This model can be shown to yield

$$\tau_q = \frac{\mu}{2}(q - q^2) \quad \zeta_p = \frac{p}{3} + \frac{\mu}{18}(3p - p^2) \tag{30}$$

where $\mu = 2\bar{m}$ is the autocorrelation exponent. Figure 8 shows the predictions of the lognormal and other models. It should be noted that despite the fact that it fits the data seemingly well for small p, the log-normal cannot be correct since for large p since it predicts that ζ_p is a decreasing function of p, which violates the incompressibility condition. As it turns out, the β-model, as well as the log-normal model are only special cases of what are known as Universal Multifractals. More details and another look at multiplicative cascades can be found in [14].

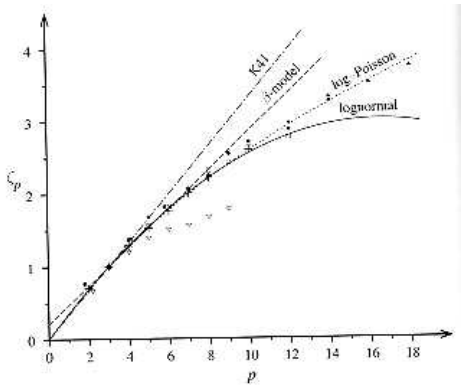

Figure 8: Comparison of the exponents ζ_p of the structure function for different models. Notice that both the K41 model and the β-model give linear relations. Experimental data from different experiments are plotted. Notice that that bending of the experimental curve at large p can be attributed to unconverged statistics. Picture taken from [3].

7.1 Universal Multifractals

In the previous section, we looked at discrete multiplicative cascades in which at each level, the larger eddies are split by a certain finite fraction. It has been shown by Schertzer and Lovejoy [15] that multifractal measures can be produced from continuous multiplicative cascades with continuous increments in the eddy size. They showed that such processes lead to the following relation for τ_q (they used $K(q) = -\tau(q)$)

$$\tau_q = \frac{-C_1}{\alpha - 1}(q^\alpha - q) \tag{31}$$

where $0 \leq \alpha \leq 2$ is called the Levy index. The case $\alpha = 1$ is marginal and yields $\tau_q = -C_1 q \ln q$. This result was given the name universal multifractals. The interesting thing to notice here is that the two multifractal models discussed above, namely the β-model and the lognormal model are contained within the framework of universal multifractals. For the β-model, we have $\alpha = 0$ and $C_1 = -\mu$. For the lognormal model, we get $\alpha = 2$ and $C_1 = \frac{-\mu}{2}$. Even more complex models such as the log-Levy model are contained within universal multifractals ($\alpha = 1.5$). Then, the universal multifractal formalism is seen to be more general. However, for $\alpha > 1$, we encounter the same problem as we did for the lognormal model, namely that ζ_p is a decreasing function of p for large enough p. This problem can seemingly be resolved by a subtle distinction between what are known as "bare" and "dressed" quantities. This leads to what is known as multifractal phase transitions [15], [16], [17].

7.2 Multifractal Phase Transitions

It was predicted by Mandelbrot in 1974 [18] that higher order moments of the dissipation will diverge when measured from a point probe. This is the starting point of the description of multifractal phase transitions. The key question in an experiment on turbulence is : What exactly does the wind probe measure? We will try to answer that question here. When a finite multiplicative cascade is generated, the field which is generated (be it the velocity or the dissipation field) is called a "bare" field. That is the quantities generated by a theoretical modeling of a finite cascade down to scale ℓ are bare quantities. However, when one collects experimental data, one is forced to use a probe of finite size, usually larger than the Kolmogorov dissipation scale. This probe then measures averages across its entire sensing area. The probe measures what are known as dressed quantities. These dressed quantities are those obtained from averaging the quantities generated by a completed cascade, that is one with an infinite number of steps. Thus, the local dissipation at scale ℓ is obtained by averaging the bare quantities over all structures of size $< \ell$. One could argue that a cascade is never complete since it cannot propagate down to $\ell = 0$ because it dissipates at small scales. However, the cascade always terminates at scales smaller than the size of the probe. The Kolmogorov scale in the atmosphere is of order of a millimeter or less while the smallest hot-wire probes are of order of a few millimeters. Thus, the probe always measures dressed data. We shall below denote bare and dressed quantities with b and d subscripts respectively. Bare quantities cannot lead to divergence of moments but dressed quantities are predicted to.

7.2.1 Analogy with Thermodynamics

As mentioned above, the functions $\tau(q)$ and $F(\alpha)$ are related to each other by a Legendre transform. It is here convenient to make the following change of variables : $\alpha - 1 \to \gamma$, $3 - F(\alpha) \to c(\gamma)$ where $c(\gamma)$ is the codimension of the singularities. Then we can write from Equation (27)

$$-\tau(q) - c(\gamma) = q\gamma \tag{32}$$

We recall that in thermodynamics a Legendre transform associates the free energy F to the entropy S as $F(T) = E - TS(E)$. We can then loosely identify γ as the energy, $c(\gamma)$ as the entropy and $\tau(q)$ as the free energy. (see [16]). In this analogy, discontinuities in the slope of $\tau(q)$ can be thought of as multifractal phase transitions. One should note that multifractal phase transitions in this description are not actual phase transitions. There is no physical observable change in the physical system. The framework is merely an analogy.

7.2.2 First Order Multifractal Phase Transitions

The singularities with very large order γ are rare events. They make up the tail of the probability distribution. Thus, one needs a very large data set to be able to reach these large orders of singularity. It was argued by [14] that for atmospheric turbulence, samples of 10^{12} data points are needed which is unattainable. However, the only data available is on atmospheric turbulence and we shall look here at the results of one experiment. It was shown in [16] that for the dressed local rate of dissipation

$$\tau_d(q) = \begin{cases} \tau(q) & q \le q_{d,crit} \\ -\gamma_{s,d} q + \Delta_s & q > q_{d,crit} \end{cases} \tag{33}$$

where $q_{d,crit}$ is the critical dressed order moment, $\gamma_{s,d}$ is the maximum reachable singularity from the finite size of the sample and $\Delta_s = d + \log N_s / \log(\ell_0/\ell)$, with N_s being the number of realizations. A realization is one set of data in the inertial range. For example, if one collects data for 60 seconds but the inertial range is valid only for structure of size smaller than $U \times 1$sec, from Taylor's hypothesis, then one would split the 60 seconds of data into 60 realizations which show scaling individually. Figure 9 below shows $K_d(q) = -\tau_d(q)$ for 4 and 704 realizations of atmospheric wind data. One can see that $K_d(q)$ becomes linear for $q > q_{d,crit} = 2.4$, thus showing apparently a first order multifractal transition.

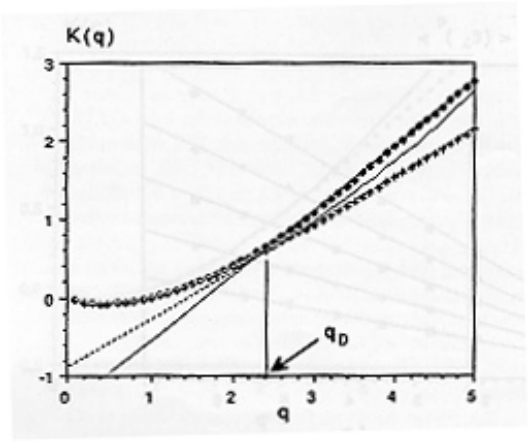

Figure 9: Empirical scaling exponent function $K(q) = -\tau(q)$ for 4 realizations(crosses) and 704 realizations (dots) compared with theoretical universal multifractal curves. Notice that there is a discontinuity in the slope at $p \approx 2.4$ and the linear slope for large p increases with the number of realization. This is a first order multifractal transition. Picture taken from [16].

7.2.3 Second Order Multifractal Phase Transitions

Second order multifractal phase transitions are postulated to be observable when the size of the sample is not large enough to reach the critical order of singularity $\gamma_{d,crit}$. Then the first order transition cannot be reached and one can show that (see [16])

$$\tau_d(q) = \begin{cases} \tau(q) & q \leq q_s \\ -\gamma_s q - \Delta_s & q > q_s \end{cases} \tag{34}$$

where $q_s = \left(\frac{\Delta_s}{C_1}\right)^{1/\alpha}$ is the critical order moment. It can be shown that Equation (34) leads to $\tau_d(q)$ being linear above q_s with a discontinuity in the second derivative at $q = q_s$, thus leading to a second order multifractal phase transition.

8 Concluding Remarks

It must be pointed out that the topics discussed in this paper are still under debate. The difficulty in performing experiments and the need for large data sets makes it still impossible to fully dismiss the K41 theory. Furthermore, there seems to be two types of experimental results. On the one hand, wind tunnel experiments allow one to have a good control over the conditions and make sure that the Taylor hypothesis is valid. But these experiments can only produce 1 or 2 decades of scaling in the power spectrum. These wind tunnel experiments seem to validate the multifractal nature of turbulence but do not show any multifractal phase transitions or divergence of moments. On the other hand, one can set up his measuring apparatus outside in a corn field and measure atmospheric turbulence and get easily 4 or 5 decades of scaling behavior. This would seem to be favorable. However, atmospheric flows are far from constant. The direction and magnitude of the r.m.s velocity are not well defined over long periods of time, thus seemingly making it difficult to justify Taylor's hypothesis. Nevertheless, the atmospheric experiments seem to validate the divergence of high order moments and the framework of multifractal phase transitions. However, these experiments might still suffer very much from finiteness of the sample size.

There is then no definite answer to the problem of turbulence. It is also very plausible that the framework of multifractals is not really valid. Some other techniques such as Renormalization Group, or closure methods might have a better chance at ultimately solving the problem of turbulence.

References

[1] Sreenivasan, K.R. *Fluid Turbulence*, Rev. Mod. Phys. **71**, S383-S395, (1999)

[2] Tritton, D.J. *Physical Fluid Dynamics*, Clarendon, Oxford, (1988)

[3] Frisch, U. *Turbulence The Legacy of A.N. Kolmogorov*, Cambridge University Press, Cambridge, (1995)

[4] Van Dyke, M. *An Album of Fluid Motion*, The Parabolic Press, Stanford, (1982)

[5] Kolmogorov, A.N. *The local structure of turbulence in incompressible viscous fluid for very large Reynolds number*, Dokl. Akad. Nauk. SSSR **30**, 9-13, (1941), (reprinted in Proc. R. Soc. Lond. A **434**, 9-13. (1991)

[6] Kolmogorov, A.N. *On degeneration (decay) of isotropic turbulence in an incompressible liquid*, Dokl. Akad. Nauk. SSSR **31**, 538-540, (1941)

[7] Kolmogorov, A.N. *Dissipation of energy in locally isotropic turbulence*, Dokl. Akad. Nauk. SSSR **32**, 16-18, (1941), (reprinted in Proc. R. Soc. Lond. A **434**, 15-17. (1991)

[8] Obukhov, A.M. *On the distribution of energy in the spectrum of turbulent flow*, Dokl. Akad. Nauk. SSSR **32**, 22-24, (1941)

[9] Obukhov, A.M. *Spectral energy distribution in a turbulent flow*, Izv. Akad. Nauk. SSSR Ser. Geogr. Geofiz. **5**, 453-466, (1941)

[10] Gouyet, J.-F. *Physics and Fractal Structures*, Masson Springer-Verlag, Paris, (1996)

[11] Kolmogorov, A.N. *A refinement of previous hypotheses concerning the local structure of turbulence in a viscous incompressible fluid at high Reynolds number*, J. Fluid Mech. **13**, 82-85, (1962)

[12] Obukhov, A.M. *Some specific features of atmospheric turbulence*, J. Fluid Mech. **13**, 77-81, (1962)

[13] Stolovistzky, G., Kailasnath, P. and Sreenivasan, K.R. *Kolmogorov's Refined Similarity Hypotheses*, Phys. Rev. Lett. **69**, 1178-1181, (1992)

[14] Meneveau, C. and Sreenivasan, K.R. *The multifractal nature of turbulent energy dissipation*, J. Fluid Mech. **224**, 429-489, (1991)

[15] Shertzer, D. and Lovejoy, S. *Physical Modeling and Analysis of Rain and Clouds by Anisotropic Scaling Multiplicative Processes*, Journal of Geophysical Research **92**, 9693-9714, (1987)

[16] Schmitt, F., Shertzer, D., Lovejoy, S. and Brunet, Y. *Empirical study of multifractal phase transitions in atmospheric turbulence*, Nonlinear Processes in Geophysics, 95-104, (1994)

[17] Schmitt, F., Lavallée, D., Shertzer, D and Lovejoy, S. *Empirical Determination of Universal Multifractal Exponents in Turbulent Velocity Fields*, Phys. Rev. Lett. **68**, 305-308, (1992)

[18] Mandelbrot, B.B. *Intermittent turbulence in self-similar cascades: divergence of high order moments and dimension of the carrier*, J. Fluid Mech. **62**, 331-358, (1974)